




## Syntheses of crystal structures and in vitro cytotoxic activities of new copper(II) complexes of pyridine-2,6-dicarboxylate

Oğuzhan Orhan, Alper Tolga Çolak, Fatih Mehmet Emen, Gorkem Kismali, Ogunc Meral, Tevhide Sel, Gülbanu Koyundereli Çilgi & Murat Taş


To cite this article: Oğuzhan Orhan, Alper Tolga Çolak, Fatih Mehmet Emen, Gorkem Kismali, Ogunc Meral, Tevhide Sel, Gülbanu Koyundereli Çilgi & Murat Taş (2015) Syntheses of crystal structures and in vitro cytotoxic activities of new copper(II) complexes of pyridine-2,6-dicarboxylate, Journal of Coordination Chemistry, 68:22, 4003-4016, DOI: [10.1080/00958972.2015.1086997](https://doi.org/10.1080/00958972.2015.1086997)

To link to this article: <http://dx.doi.org/10.1080/00958972.2015.1086997>

 View supplementary material 

 Accepted author version posted online: 27 Aug 2015.  
Published online: 16 Sep 2015.


 Submit your article to this journal 

 Article views: 138

 View related articles 

 View Crossmark data 

## Syntheses of crystal structures and *in vitro* cytotoxic activities of new copper(II) complexes of pyridine-2,6-dicarboxylate

OĞUZHAN ORHAN<sup>†</sup>, ALPER TOLGA ÇOLAK\*<sup>†</sup>, FATİH MEHMET EMEN<sup>‡</sup>,  
GORKEM KISMALI<sup>§</sup>, OGUNC MERAL<sup>§</sup>, TEVHİDE SEL<sup>§</sup>,  
GÜLBANU KOYUNDERELI ÇILGI<sup>¶</sup> and MURAT TAŞI<sup>1</sup> 

<sup>†</sup>Faculty of Arts and Sciences, Department of Chemistry, Dumlupınar University, Kütahya, Turkey

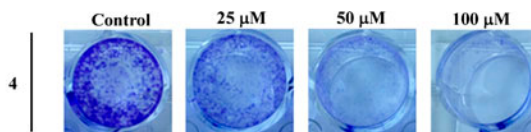
<sup>‡</sup>Faculty of Arts and Sciences, Department of Chemistry, Mehmet Akif Ersoy University, Burdur, Turkey

<sup>§</sup>Faculty of Veterinary Medicine, Department of Biochemistry, Ankara University, Ankara, Turkey

<sup>¶</sup>Faculty of Technology, Department of Material Science and Engineering, Pamukkale University, Denizli, Turkey

<sup>1</sup>Science Faculty, Department of Chemistry, Giresun University, Giresun, Turkey

(Received 12 March 2015; accepted 14 August 2015)



[Cu(pydc)(im)]<sub>n</sub> (1), [Cu(pydc)(mim)<sub>3</sub>]·2H<sub>2</sub>O (2), [Cu(pydc)(ampy)(H<sub>2</sub>O)]·H<sub>2</sub>O (3), and [Cu(pydc)(phen)][Cu(Hpydc)<sub>2</sub>] (4) (H<sub>2</sub>pydc = 2,6-pyridinedicarboxylic acid or dipicolinic acid, im = imidazole, mim = 2-methylimidazole, ampy = 2-amino-4-methylpyridine, and phen = 1,10-phenanthroline) were synthesized and characterized by elemental analysis, spectroscopic measurements (UV–vis and IR spectra) and single crystal X-ray diffraction. Complexes 1, 2 and 3 were studied by thermogravimetric analysis from ambient temperature to 1100 K under nitrogen and thermal stabilities were investigated. The effects of complexes on proliferation of fibrosarcoma cells were investigated using the Quick Cell Proliferation Assay. The cell viability changes depend on the concentrations and type of complexes. According to cell proliferation/viability data, 4 was determined to be the most cytotoxic.

**Keywords:** 2,6-Pyridinedicarboxylate; Crystal structure; Cytotoxic activity; Kinetic analysis

### 1. Introduction

Metal-based drugs have existed for decades and cisplatin is one of the most effective antitumor drugs. However, cisplatin-based chemotherapy leads to severe side effects that restrict

\*Corresponding author. Email: [tolga.colak@dpu.edu.tr](mailto:tolga.colak@dpu.edu.tr)

<sup>1</sup>Present address: Education Faculty, Department of Science Education, Ondokuz Mayıs University, Samsun, Turkey.

its clinical use. Therefore, many laboratories have been synthesizing and characterizing new potential metal-based anticancer drugs to reduce toxicity and improve clinical effectiveness [1, 2]. Metal-based compounds containing titanium, copper, ruthenium, tin, and rhodium have been reported to possess promising chemotherapeutic potential, and they have different mechanisms of action compared to platinum-based drugs [2–7]. Copper is an essential element for normal human metabolism. In biological systems, copper exists as a variety of complexes as coordinated forms of copper are more stable than the corresponding ionic species [8]. Several families of copper complexes comprising different ligands demonstrated notable anticancer activity [9–15]. Our choice of imidazole and pyridine derivatives is based on differences in their DNA binding ability. Nitrogen heterocycles have recently been reported to exhibit therapeutic anticancer and antimicrobial activities [16]. The binding of copper ions to specific sites can modify the conformational structures of proteins, polynucleotides, DNA, and bio-membranes. The binding of Cu to DNA occurs with high affinity [17–19]. The effects of such copper(II) complexes are known [20, 21]. In view of the excellent coordination capability of 2,6-pyridinedicarboxylic acid, we used 2,6-pyridinedicarboxylic acid as an organic building block to construct multidimensional supramolecular networks expecting that the group may generate covalent, hydrogen bonding, and/or  $\pi$ - $\pi$  stacking interactions with transition metal ions in the assembly [22–28]. Dipicolinic acid is a natural compound involved in metal chelation reactions responsible for the thermal resistance in bacteria spores and the activation or inhibition of metalloenzymes. This amino diacid has molecular structure and peculiar coordination chemistry influenced by its constrained planar conformation [29]. The coordination of carboxylate anions to Cu(II) cations has been extensively studied and the ability of Cu(II) to adopt a variety of chromophores has been demonstrated [30]. Based on the structure of anticancer platinum complexes, dicarboxylates are being used as active species in anticancer studies instead of chlorides [31]. There are limited anticancer studies in the literature performed by copper(II) complexes obtained from dicarboxylate ligands [32–34]. Likewise, there is no anticancer study performed by Cu(II) complexes obtained from pyridine-2,6-dicarboxylate. Moreover, based on the soft and hard acid base theory, borderline acid  $\text{Cu}^{2+}$  ion could coordinate with O and N groups [35]. In the present study, we describe the synthesis, spectroscopic and thermal analysis, crystal structure, and anticancer activities of  $[\text{Cu}(\text{pydc})(\text{im})_n]$  (**1**),  $[\text{Cu}(\text{pydc})(\text{mim})_3] \cdot 2\text{H}_2\text{O}$  (**2**) and  $[\text{Cu}(\text{pydc})(\text{ampy})(\text{H}_2\text{O})] \cdot \text{H}_2\text{O}$  (**3**). Single crystal values of **4** were not good. However, these poor crystal values offered us valuable information about the structure of **4**. Moreover, it is characterized by IR, UV–vis, magnetic susceptibility and elemental analysis. Furthermore, the compound has cancer activity.

## 2. Experimental studies

### 2.1. Materials and measurements

All chemicals and solvents used for the syntheses were of reagent grade. Pyridine-2,6-dicarboxylic acid, imidazole, 2-methylimidazole, or 2-amino-4-methylpyridine, 1,10-phenanthroline,  $\text{C}_2\text{H}_5\text{OH}$  and  $\text{Cu}(\text{CH}_3\text{COO})_2 \cdot \text{H}_2\text{O}$  (Aldrich) were used as received. Elemental analyses (C, H and N) were performed using a Vario EL III CHNS elemental analyzer. Magnetic susceptibility measurements were performed at room temperature using a Sherwood Scientific MK1 model Gouy magnetic balance. UV–vis spectra were obtained in DMSO

solutions ( $10^{-3}$  mol L $^{-1}$ ) of the complexes with a Shimadzu Pharmaspec UV-1700 spectrometer from 1000 to 190 nm. FT-IR spectra were recorded from 4000 to 400 cm $^{-1}$  with a Bruker Optics, Vertex 70 FT-IR spectrometer using KBr pellets. All thermogravimetry (TG), differential thermogravimetry (DTG), and differential thermal analysis (DTA) curves were obtained simultaneously using a Shimadzu DTG-60H thermal analyzer. The measurements were carried out in flowing nitrogen (100 mL min $^{-1}$ ) from 300 to 1000 K in an alumina crucible using 10 °C min $^{-1}$  heating rate. Highly sintered Al $_2$ O $_3$  was used as the reference material. The sample mass ( $w_0$ ) ranged from 4 to 5 mg. The melting points of indium and tin provided by Shimadzu were used to calibrate the temperature.

## 2.2. Crystallographic analyses

Single crystal X-ray data were collected on an Agilent SuperNova diffractometer with an Eos CCD detector using Mo K $\alpha$  radiation ( $\lambda = 0.71073$  Å). The CrysAlisPro software was used for data collection, cell refinement, and data reduction. Using Olex2 [36], the structures were solved by the ShelXS [37] structure solution program by direct methods and refined by ShelXL [37] refinement package using the least-squares minimization. Olex2

Table 1. Summary of crystallographic data and structure refinement results for **1–3**.

Identification code	<b>1</b>	<b>2</b>	<b>3</b>
Empirical formula	C $_{10}$ H $_7$ CuN $_3$ O $_4$	C $_{19}$ H $_{25}$ CuN $_7$ O $_6$	C $_{13}$ H $_{15}$ CuN $_3$ O $_6$
Formula weight	296.73	511.00	372.82
Temperature (K)	293(2)	293(2)	293(2)
Crystal system	Monoclinic	Monoclinic	Orthorhombic
Space group	<i>Cc</i>	<i>P2/c</i>	<i>Pccn</i>
<i>a</i> (Å)	8.187(5)	15.089(5)	13.3117(7)
<i>b</i> (Å)	12.67(3)	9.905(5)	14.4931(7)
<i>c</i> (Å)	9.766(6)	15.754(5)	15.1774(7)
$\alpha$ (°)	90	90.000(5)	90
$\beta$ (°)	91.60(9)	96.938(5)	90
$\gamma$ (°)	90	90.000(5)	90
Volume (Å $^3$ )	1013(2)	2337.3(16)	2928.1(2)
<i>Z</i>	4	4	8
$\rho_{\text{calcd}}$ (mg mm $^{-3}$ )	1.946	1.452	1.691
$\mu$ mm $^{-1}$	2.168	0.983	1.528
<i>F</i> (0 0 0)	596.0	1060.0	1528.0
Crystal size (mm $^3$ )	0.185 × 0.193 × 0.201	0.121 × 0.176 × 0.214	0.148 × 0.170 × 0.237
Radiation	Mo K $\alpha$ ( $\lambda = 0.7107$ )	Mo K $\alpha$ ( $\lambda = 0.7107$ )	MoK $\alpha$ ( $\lambda = 0.71073$ )
2 $\theta$ range	6.43–51.488°	6.932–52.878°	6.79–55.41°
Index ranges	–6 ≤ <i>h</i> ≤ 10, –15 ≤ <i>k</i> ≤ 14, –11 ≤ <i>l</i> ≤ 11	–18 ≤ <i>h</i> ≤ 18, –12 ≤ <i>k</i> ≤ 7, –19 ≤ <i>l</i> ≤ 17	–17 ≤ <i>h</i> ≤ 10, –11 ≤ <i>k</i> ≤ 17, –9 ≤ <i>l</i> ≤ 19
Reflections collected	1883	8610	7644
Independent reflections	1217 [ $R_{\text{int}} = 0.0538$ , $R_{\text{sigma}} = 0.1277$ ]	4377 [ $R_{\text{int}} = 0.0595$ , $R_{\text{sigma}} = 0.1324$ ]	2946 [ $R_{\text{int}} = 0.0406$ , $R_{\text{sigma}} = 0.0566$ ]
Data/restraints/ parameters	1217/2/67	4377/6/144	2946/0/214
Goodness-of-fit on $F^2$	0.809	1.042	1.148
Final $R$ indexes [ $I > 2\sigma(I)$ ]	$R_1 = 0.0511$ , $wR_2 = 0.0811$	$R_1 = 0.1223$ , $wR_2 = 0.3068$	$R_1 = 0.0589$ , $wR_2 = 0.1237$
Final $R$ indexes [all data]	$R_1 = 0.0995$ , $wR_2 = 0.0900$	$R_1 = 0.1980$ , $wR_2 = 0.3471$	$R_1 = 0.0818$ , $wR_2 = 0.1342$
Largest diff. peak/hole (eÅ $^{-3}$ )	0.65/–0.38	1.84/–2.15	0.56/–0.42

was used to prepare the material for publication. All hydrogens were refined using a riding model. The details of the X-ray data collection, structure solution, and structure refinement are given in table 1. Selected bond distances and angles are listed in tables S1–S3.

### 2.3. Preparation of complexes

[Cu(pydc)(im)]<sub>n</sub> (**1**), [Cu(pydc)(mim)<sub>3</sub>] $\cdot$ 2H<sub>2</sub>O (**2**), [Cu(pydc)(ampy)(H<sub>2</sub>O)] $\cdot$ H<sub>2</sub>O (**3**), and [Cu(pydc)(phen)][Cu(Hpydc)<sub>2</sub>] (**4**).

A solution of H<sub>2</sub>pydc (1.0 mmol 0.167 g) in water (30 mL) was added dropwise with stirring at room temperature to a solution of Cu(CH<sub>3</sub>COO)<sub>2</sub> $\cdot$ H<sub>2</sub>O (1.0 mmol, 0.20 g) in water (40 mL). The solution immediately became a suspension and was stirred for 2 h at reflux. Then the imidazole (3 mmol, 0.20 g) for **1** or 2-methylimidazole (3 mmol, 0.25 g) for **2** or 2-amino-4-methylpyridine (3 mmol, 0.32 g) for **3** or 1,10-phenanthroline (3 mmol, 0.54 g) for **4** in ethanol (40 mL) was added dropwise to this suspension. The clear blue solutions were stirred for 24 h at room temperature. Approximately two months later, the formed crystals were filtered and washed with 50 mL of cold ethanol and dried in air. *Analytical data*: C<sub>10</sub>H<sub>7</sub>CuN<sub>3</sub>O<sub>4</sub> for **1** (296.73 g mol<sup>-1</sup>) = Calcd C 40.48, H 2.38, N 14.16, Cu 21.42; found C 41.15, H 2.21, N 13.93, Cu 21.10. Yield 44%, *Analytical data*: C<sub>19</sub>H<sub>25</sub>CuN<sub>7</sub>O<sub>6</sub> for **2** (511.0 g mol<sup>-1</sup>) = Calcd C 44.66, H 4.93, N 19.19, Cu 12.44; found C 44.19, H 4.80, N 18.96, Cu 12.13. Yield 68%. *Analytical data*: C<sub>13</sub>H<sub>15</sub>CuN<sub>3</sub>O<sub>6</sub> for **3** (372.82 g mol<sup>-1</sup>) = Calcd C 41.88, H 4.06, N 11.27, Cu 17.04; found C 41.65, H 3.91, N 11.20, Cu 16.81, Yield 34%, *Analytical data*: C<sub>33</sub>H<sub>19</sub>Cu<sub>2</sub>N<sub>5</sub>O<sub>12</sub> for **4** (805.62 g mol<sup>-1</sup>) = Calcd C 49.20, H 2.50, N 8.69, Cu 15.78; found C 48.76, H 2.69, N 8.21, Cu 16.10, Yield 14%.

## 3. Results and discussion

### 3.1. FT-IR spectra, UV-vis spectra and magnetic susceptibilities

The broadbands at 3437, 3340, and 3355 cm<sup>-1</sup> are attributed to  $\nu$ (OH) of free water molecules and as aqua ligand for **2** and **3**, respectively. The absorption peaks at 3104 and 3134 cm<sup>-1</sup> are assigned to  $\nu$ (NH) stretches of im and mim in **1** and **2**, respectively. The absorption peak at 3221 cm<sup>-1</sup> is attributed to  $\nu$ (NH<sub>2</sub>) of ampy ligand in **3**. In the middle energy range, 2930, 2953, 3072, and 2970 cm<sup>-1</sup> absorptions originate from  $\nu$ (CH) for **1**, **2**, **3**, and **4**, respectively. The strong absorption bands at 1661, 1606, 1626, and 1614 cm<sup>-1</sup> are due to  $\nu$ (C=C)+ $\nu$ (C=N) of ligands for **1**, **2**, **3**, and **4**, respectively. In the spectra free H<sub>2</sub>pydc [38] disappeared and a new carboxylate band  $\nu_s$ (COO<sup>-</sup>) appeared at 1363 cm<sup>-1</sup> for **1**, 1360 cm<sup>-1</sup> for **2**, 1349 cm<sup>-1</sup> for **3**, and 1368 cm<sup>-1</sup> for **4**, indicating that the carboxylic group of H<sub>2</sub>pydc participate in coordination with copper(II) through deprotonation. Several  $\nu_{as}$ (COO<sup>-</sup>) strong bands in free H<sub>2</sub>pydc are shifted to lower frequencies 1596, 1565, 1561, and 1582 cm<sup>-1</sup> in **1**, **2**, **3**, and **4**, respectively. The difference between the asymmetric and symmetric carboxylate stretch ( $\Delta = \nu_{as}(\text{COO}^-) - \nu_s(\text{COO}^-)$ ) is often used for interpretation of infrared spectra with the structures of metal carboxylates [39]. These values are approximately 228 cm<sup>-1</sup>, typical of monodentate carboxylate groups [40]. These differences were determined as  $\Delta = 233$  cm<sup>-1</sup> (1596–1363 cm<sup>-1</sup>, monodentate) for **1**,  $\Delta = 205$  cm<sup>-1</sup> (1565–1360 cm<sup>-1</sup>, monodentate) for **2**,  $\Delta = 212$  cm<sup>-1</sup> (1561–1349 cm<sup>-1</sup>, monodentate) for

**3**, and  $\Delta = 214 \text{ cm}^{-1}$  ( $1582\text{--}1368 \text{ cm}^{-1}$ , monodentate) for **4**. The absorptions at 548, 526, 553, and  $527 \text{ cm}^{-1}$  correspond to Cu–O vibration and the bands at 431, 464, 439, and  $429 \text{ cm}^{-1}$  are attributed to Cu–N vibrations of **1**, **2**, **3**, and **4**, respectively. The electronic spectra of **1**, **2**, and **4** in DMSO show broad absorption at 753, 755, and 776 nm, respectively, which can be attributed to  ${}^2B_{1g} \rightarrow {}^2E_g$ ,  ${}^2B_{1g} \rightarrow {}^2B_{2g}$  and  ${}^2B_{1g} \rightarrow {}^2A_{1g}$  transitions ( $\epsilon = 45, 38$  and  $90 \text{ L mol}^{-1} \text{ cm}^{-1}$ , respectively). This broad absorption suggests the existence of distorted octahedral geometry as expected from the Jahn–Teller effect in six-coordinate  $d^9$  metal ions in **1**, **2**, and **4**. The electronic spectrum of **3** in DMSO exhibits absorption centered at 777 ( $\epsilon = 123 \text{ L mol}^{-1} \text{ cm}^{-1}$ ), which corresponds to d–d transitions. These values were attributed to  $d_{xz}, d_{yz} \rightarrow d_{x^2-y^2}$  ( $a_1 \rightarrow b_1$ ) transition, which lie within one broad envelope. The  $\Delta_o$  values for the complexes were calculated as 13,280, 13,245, 12,870, and  $12,886 \text{ cm}^{-1}$  for **1**, **2**, **3**, and **4**, respectively. The  $\Delta_o$  value of **1** is higher than that of **2**, **3**, and **4** as polymeric im is a stronger field ligand than mim and ampy ligands. **1**, **2**, **3**, and **4** exhibit magnetic moment values of 1.60, 1.95, 1.73, and 3.00 (1.50 for per Cu ion) BM, respectively, which correspond to one unpaired electron. The suggested structure is illustrated in figure 1 in light of these data.

### 3.2. Thermal analysis

Figure S1 shows the TG, DTA, and DTG curves of **1**, **2**, and **3**. While **1** decomposes in two consecutive stages, **2** and **3** decompose in four consecutive stages. All complexes yield CuO residue. The decomposition temperature range, DTA peak positions, percentage of mass losses (experimental and theoretical) and evolved moieties of the decomposition reactions are summarized in table 2. The suggested decomposition mechanisms of **1**, **2**, and **3** are illustrated in scheme 1.

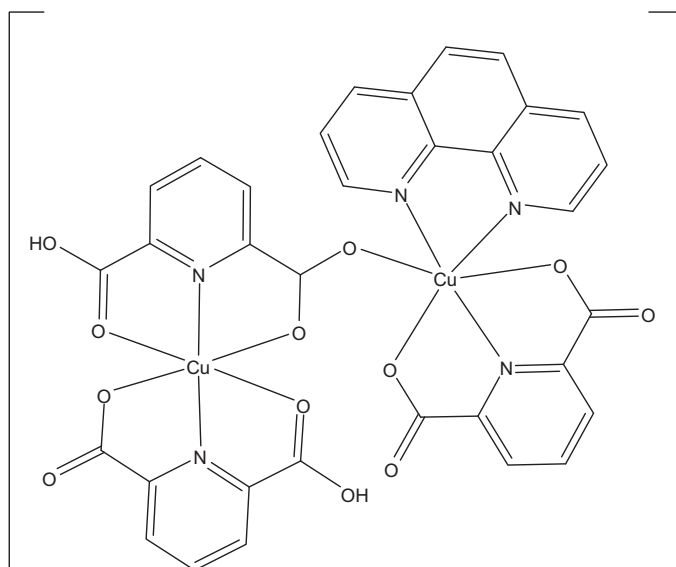


Figure 1. Proposed structure for  $[\text{Cu}(\text{pydc})(\text{phen})][\text{Cu}(\text{Hpydc})_2]$  (**4**).

Table 2. Thermoanalytical results of the decomposition reactions of **1**, **2**, and **3**.

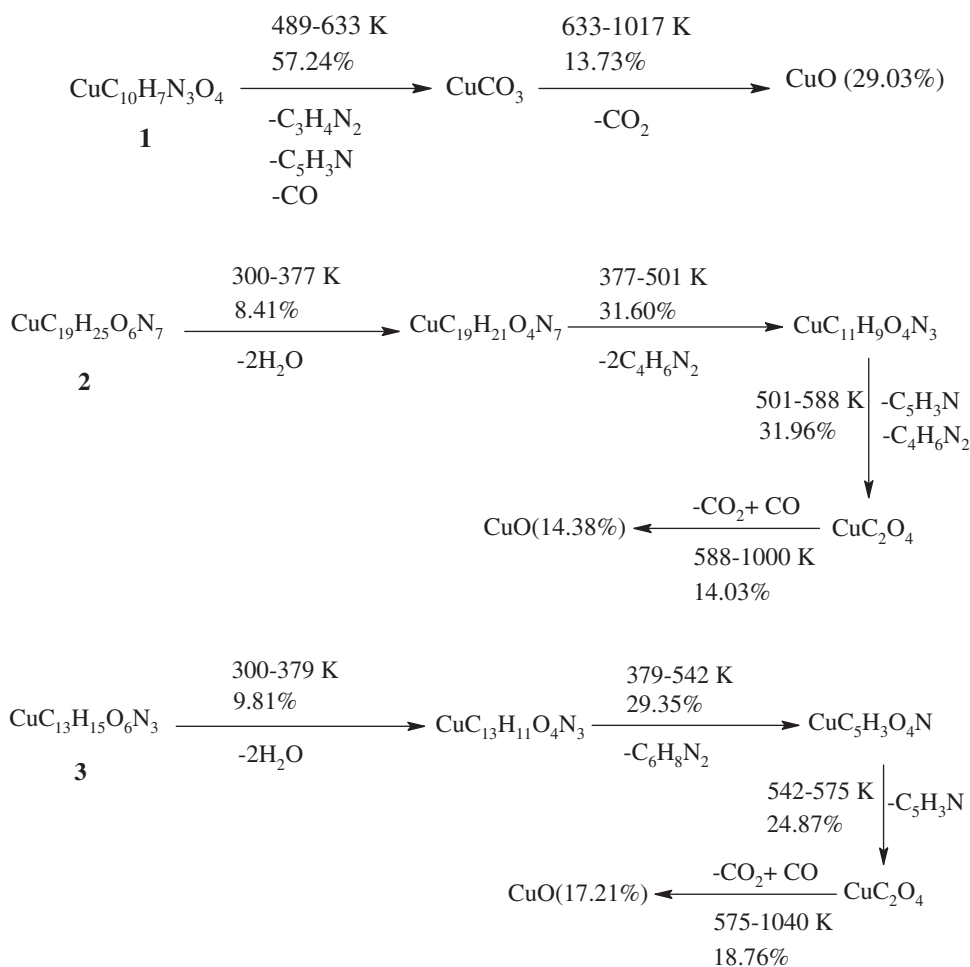
Sample	Stage	DTA peak (K)	TG temp. range (K)	Mass loss (%)		Evolved moiety
				Exp.	Theo.	
1	I	579	489–633	57.24	58.30	$-\text{C}_5\text{H}_8\text{N}_2 + \text{C}_5\text{H}_3\text{N} + \text{CO}$
	II	–	633–1017	13.73	13.82	$-\text{CO}_2$
	Residue (CuO)	–	–	29.03	27.88	–
2	I	357	300–377	8.41	7.05	$-2\text{H}_2\text{O}$
	II	480	377–501	31.60	31.70	$\text{C}_4\text{H}_6\text{N}_2$
	III	565	501–588	31.96	31.42	$\text{C}_4\text{H}_6\text{N}_2 +$
	IV	–	588–1000	14.03	14.10	$\text{C}_5\text{H}_3\text{N}$
	Residue (CuO)	–	–	14.38	15.55	$-\text{CO}_2 + \text{CO}$
3	I	347	300–379	9.81	9.66	$-2\text{H}_2\text{O}$
	II	541	379–542	29.35	28.96	$-\text{C}_6\text{H}_8\text{N}_2$
	III	576	542–575	24.87	22.22	$-\text{C}_5\text{H}_3\text{N}$
	IV	–	575–1040	18.76	21.32	$-\text{CO}_2 + \text{CO}$
	Residue (CuO)	–	–	17.21	17.84	–

### 3.3. Description of the crystal structures

**3.3.1. [Cu(pydc)(im)]<sub>n</sub> (1).** Crystallographic data of the complexes are summarized in table 2. Selected bond lengths and angles are given in table S4. Molecular structures, intermolecular interactions, and packing diagrams are shown in figures 2, 3 and S5. The asymmetric unit of **1** contains a pydc and an im ligand. The pydc ligands are tridentate bonding to the metal using its pyridine and O1 and O3 of its two carboxylate groups, in dianionic form, giving [Cu(pydc)(im)] complex units. The remaining oxygens (O2 and O4) are free for bonding to Cu(II) ions at related symmetry to complete octahedral environment around the metal (figure 2).

The molecules in the asymmetric units formed polymeric sheets by interactions of intermolecular hydrogen bonds (figure S5). To form infinite polymeric sheets, N3 and C9 of the imidazole ring formed hydrogen bonds with O2<sup>i</sup> and O4<sup>ii</sup> of pydc, respectively. To contribute to the formation of polymeric chain the pydc ring acted as hydrogen bond donors using its C3 and C5 to O4<sup>iii</sup> and O2<sup>iv</sup>, respectively (i):  $1/2 + x, 1/2 - y, 1/2 + z$ , (ii):  $-1/2 + x, 1/2 - y, -1/2 + z$ , (iii):  $-1/2 + x, -1/2 - y, -1/2 + z$ , (iv):  $1/2 + x, -1/2 - y, 1/2 + z$ . Therefore, the 2-D polymeric sheets lie parallel to the [1 0 1] plane. Between the parallel sheets, the Cu(II) ions were coordinated by O2<sup>v</sup> and O4<sup>vi</sup> of pydc at  $x, -y, 1/2 + z$  and  $x, -y, -1/2 + z$  to form distorted octahedral environment around the metal centers and 1-D coordination polymer along the *c* axis (figure 3). There were also  $\pi \cdots \pi$  interactions between the im ring and pyridine ring between the sheets parallel to the others at  $1/2 + x, 1/2 + y, z$  and  $-1/2 + x, -1/2 + y, z$  symmetries (figure S5).

**3.3.2. [Cu(pydc)(mim)<sub>3</sub>]·2H<sub>2</sub>O (2).** Compound **2** crystallizes in the monoclinic space group *P2<sub>1</sub>/c*. Selected bond lengths and angles are given in table S5. The dianionic pydc ligand bonds in tridentate. The mim ligands coordinated via their nitrogens. In the MN<sub>4</sub>O<sub>2</sub> highly distorted octahedral geometry, the equatorial plane of the octahedron was created by nitrogens of the ligands and axial positions were occupied by carboxylate oxygens of pydc (figure 4). The planes of the carboxyl groups were not parallel to the pyridine ring plane as the angles between the planes were 18.171° and 15.547° for O1–C1–O2 and O3–C7–O4

Scheme 1. The suggested decomposition mechanisms of **1**, **2**, and **3** on the basis of the thermal analysis data.

planes, respectively. All the 2-methylimidazole rings were nearly perpendicular to each other and an intramolecular C–H– $\pi$  interaction was detected between the methyl of mim and im ring of mim (figure 4). The NH of the mim ligands form intramolecular hydrogen bonds with the O4– and O2– of pydc ligands (figure 5 and table S5). The complexes extend to form an infinite polymeric chain parallel to the [0 0 1] plane by N3–H3–O4 and N7–H7–O2 hydrogen bonds at  $2 - x$ ,  $1 - y$ ,  $1 - z$  and  $1 - x$ ,  $-y$ ,  $1 - z$ , respectively (figures 4 and 5, table S5).

To bond the polymeric chains to each other, the chain of hydrate water acted as a bridge by the formation of N5–H5–O5 and O5–H5c–O1 hydrogen bonds between the mim ring nitrogen and water molecules (figure 4). Also C17 of mim formed a C–H– $\pi$  interaction with the ring of mim at  $x$ ,  $-1 + y$ ,  $z$  symmetry (figure 5). Thus, the molecules showed infinite 3-D molecular networks parallel to the [1–10], [0 2 1] and [1–11] planes.



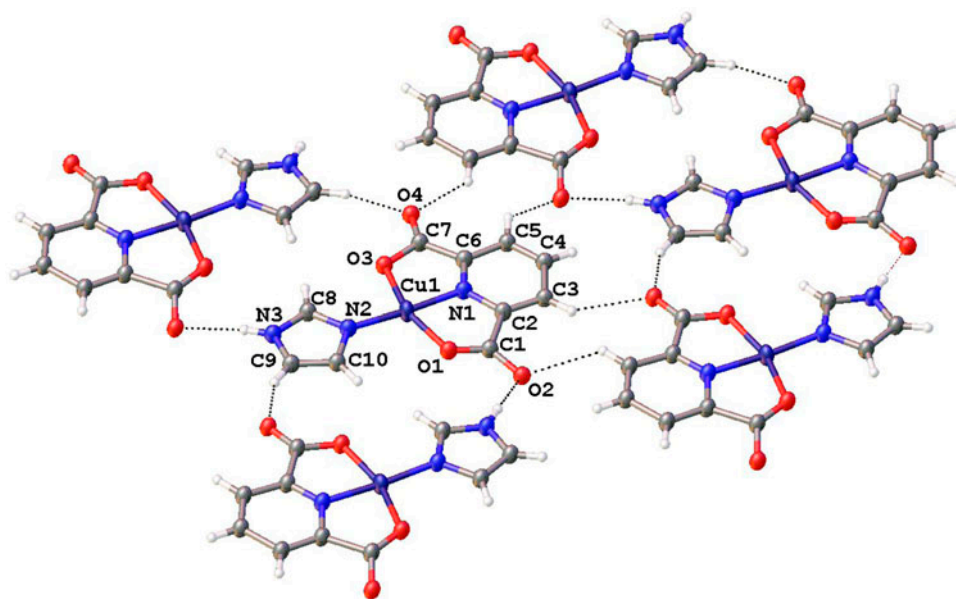


Figure 2. The asymmetric unit showing labeled atoms of **1** and formation of a sheet.

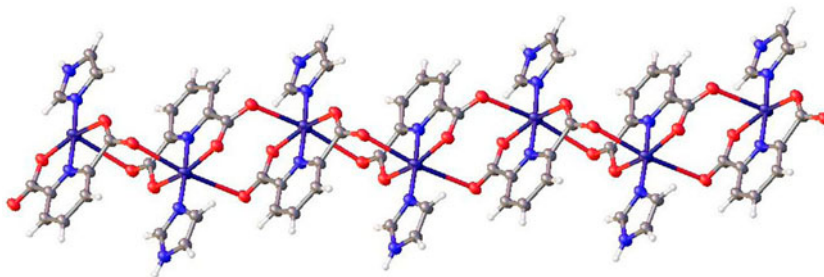


Figure 3. The coordination polymer structure of **1**.

**3.3.3. [Cu(pydc)(ampy)(H<sub>2</sub>O)]·H<sub>2</sub>O (**3**).** Compound **3** has pydc, ampy, and water ligands to form square-pyramidal geometry around copper. Furthermore, the complex has a hydrate water (figure 6). Selected bond lengths and angles are given in table S6. The pydc is tridentate bonding by its two carboxylate oxygens and pyridine ring nitrogen in di-anionic form. Both pyridine rings were nearly in the plane of the pyramid and all the substituents were nearly in the ring planes. The ampy ligand formed an intramolecular hydrogen bond using its C8 and amine nitrogen with coordinated oxygens (figure 7). Ampy Cg(3) [1] → Cg(4) [5665.01] 3.577(3) 1 - x, 1 - y, -z. Pydc Cg(4) [1] → Cg(3) [5665.01] 3.577(3) 1 - x, 1 - y, -z.

Complex units formed 2-D molecular sheets by formation of N3-H3 O6, C4-H4-O1, and O6-H6a-O4 hydrogen bonds (figure S6). Oxygen of pydc and hydrogen bonds formed by hydrate water molecules bind aqua ligands of sheets to each other (figure S6). Also, the

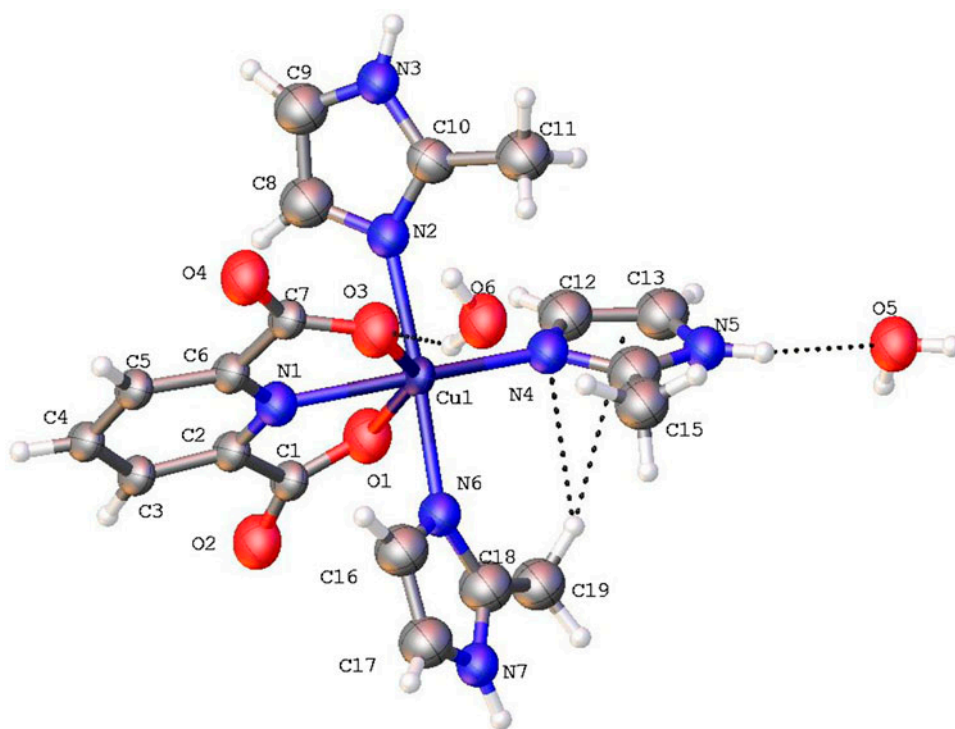


Figure 4. The structure of 2.

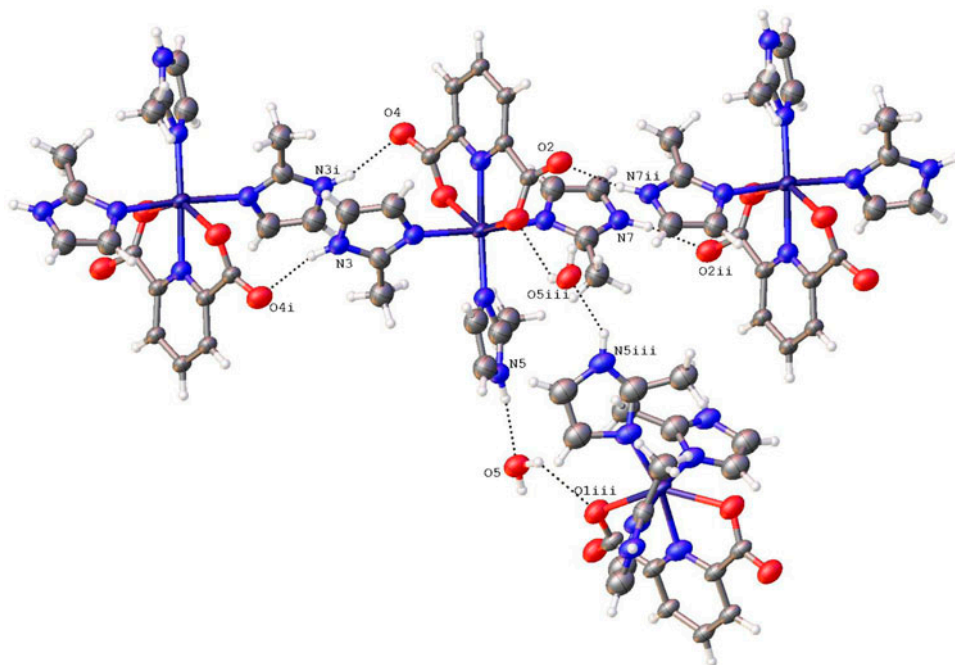


Figure 5. The formation of polymeric chain by the N-H...O hydrogen bonds in 2.

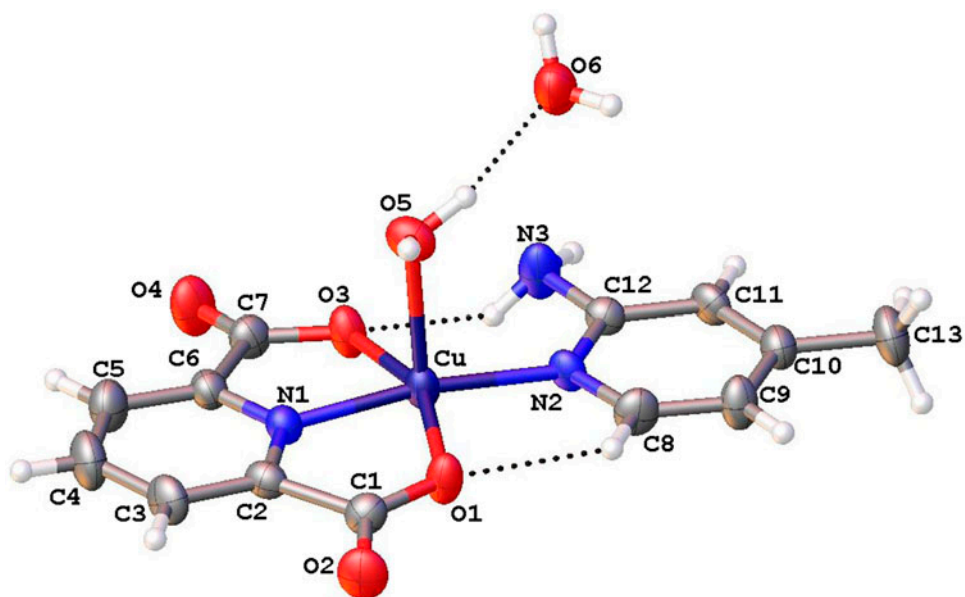


Figure 6. The structure of 3.

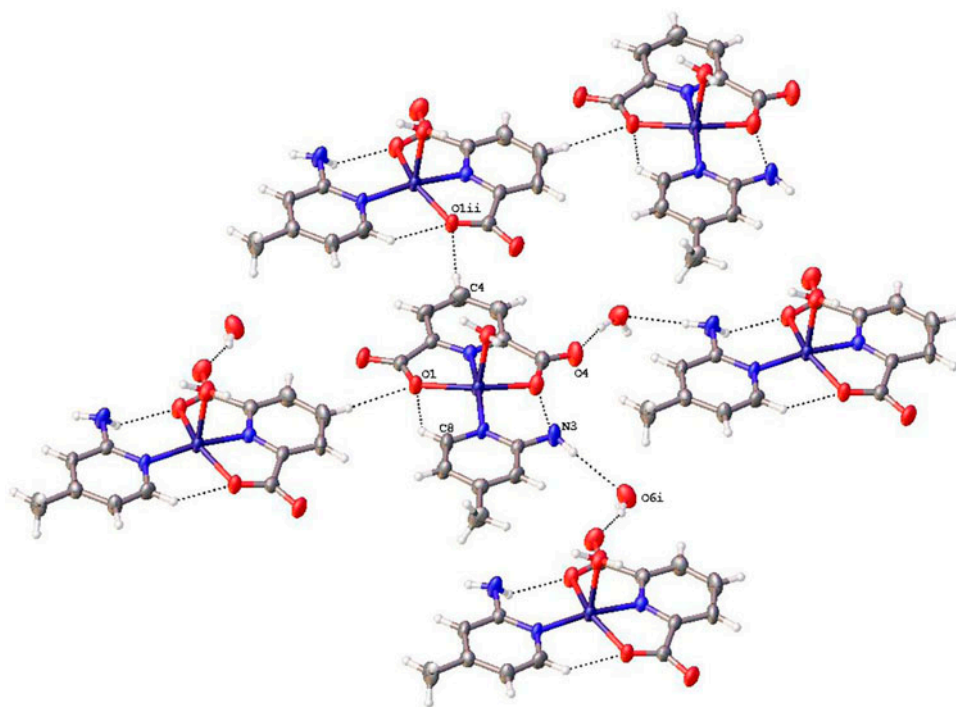


Figure 7. The formation of 2-D molecular sheets for 3.

sheets were bonded via formation of O6–H6b–O2 hydrogen bonds between the hydrate water molecules and O2 of pydc;  $\pi \cdot \cdot \pi$  interactions between pydc and ampy ring contributed to bonding of the sheets. Thus, 3-D supramolecular network occurred.

### 3.4. Discussion and conclusion of cytotoxic and anticancer effects of complexes

The effects of complexes on the proliferation of fibrosarcoma cells were investigated using the Quick Cell Proliferation Assay. The cell viability changes were found to depend on the concentrations and type of complexes. Results are shown in figures S7–S9. Complexes inhibited the proliferation of HT-1080 human fibrosarcoma cells in a concentration-dependent manner. Half maximal inhibitory concentration ( $IC_{50}$ ) values were determined for 24 h incubation. All the complexes were dissolved in water for injection. According to cell proliferation/viability data, **4** was determined to be the most cytotoxic (figure S10).

Cell membrane damage was also monitored using the LDH leakage assay because LDH is a stable cytosolic enzyme in normal cells and can leak into the extracellular fluid only after membrane damage. Exposure to complexes at different doses for 24 h resulted in LDH release from cells to varying extents. Supernatant LDH levels (IU/mL) are provided in figure S7. Treatment of **4** resulted in a remarkable increase in LDH release, as a cell damage marker. According to cytotoxicity assays, **4** was most active so other assays were performed with complex **4**. We observed several picnotic nuclei, anisonucleosis, and nuclear condensation in cells treated with different concentrations of **4**. This nuclear morphological change precedes chromatin condensation and can be dissociated from many early apoptotic events, such as DNA cleavage and cell shrinkage (figure 8). The clonogenic cell survival assay determines the ability of a cell to proliferate indefinitely, thereby retaining its reproductive ability to form a large colony. We observed a significant decrease on colony formation after seven days on complex **4** treated cells (figure 9). Within the past decade, copper complexes were used for therapy or diagnosis of cancer. Most of them were applied for the treatment of various cancer types like breast, lung, colon, kidney, prostate, human squamous cervix carcinoma, endometrial and ovarian carcinoma, melanoma-skin, renal carcinoma, non-Hodgkin's lymphoma, human osteogenic sarcoma, malignant melanoma, and mammary gland cancer [41]. Wani *et al.* reported that oxopyrrolidine-based ligand and its copper(II), nickel(II), and ruthenium(III) complexes showed moderate anti-cancer activities on MCF-7 (wild type) breast cancer cell lines [42]. Li *et al.* reported that water-soluble mononuclear Cu(II) complex showed considerable cytotoxic activity against HeLa cells, better than cisplatin [43]. Subha *et al.* reported that binary and mixed ligand Cu (II) complexes containing amino acid Schiff base and heterocyclic nitrogen co-ligands, imidazole, and pyridine had cytotoxic effects on breast cancer cell lines (MCF-7) [44]. Zhao

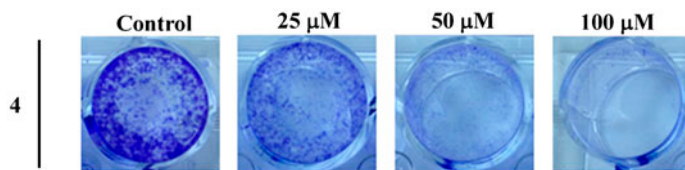


Figure 8. Clonogenic assay of HT-1080 cell line performed in 12 well plates. Cells were treated with **4** for seven days. (A) Control, (B) 25  $\mu$ M, (C) 50  $\mu$ M and (D) 100  $\mu$ M.

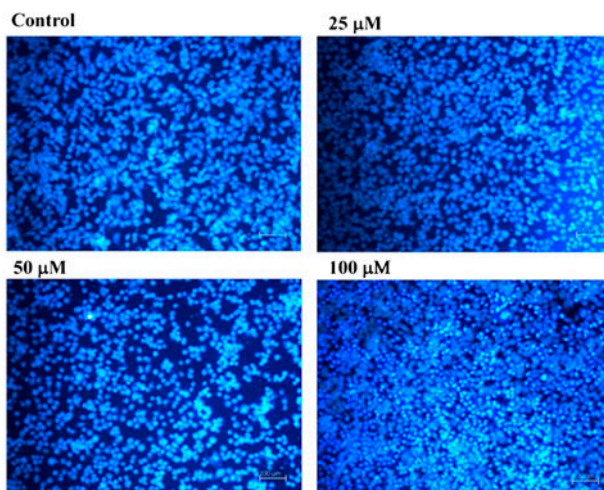


Figure 9. DAPI nuclear staining for **4**. (A) Control, (B) 25  $\mu\text{M}$ , (C) 50  $\mu\text{M}$  and (D) 100  $\mu\text{M}$ ; 24 h incubation.

*et al.* reported that copper(II)-based complexes had cytotoxic effects on several human alimentary system carcinoma cell lines (SGC7901, EC109, SMMC7721, and HT29) [45]. The differences in the antiproliferative effects of **1**, **2**, **3**, and **4** indicate that the pyridine-2,6-dicarboxylate complexes have different antiproliferative activities on fibrosarcoma cell line. Consequently, our data based on clonogenic and quick cell proliferation assay demonstrate that **4** is very active with higher antiproliferative effects than the other complexes. Targeting apoptosis or autophagy is a promising strategy for cancer drug discovery. The present data will aid in future work. In investigating the agents that trigger programmed cell death, the sensitivity of tumor cells indicates the success of chemotherapies and the reduced costs of treatment. Thus, this study provides strong evidence that **4** is a promising new compound. Further mechanistic and *in vivo* studies are needed to better understand the metabolic effects of this compound.

### Supplementary material

CCDC-988051, 988052 and 988053 contains the supplementary crystallographic data for **1–3**. These data can be obtained free of charge via <http://www.ccdc.cam.ac.uk/conts/retrieving.html> or from the Cambridge Crystallographic Data Center, 12 Union Road, Cambridge CB2 1EZ, UK; Fax:+44 1223 336 033; or E-mail: [deposit@ccdc.cam.ac.uk](mailto:deposit@ccdc.cam.ac.uk).

### Disclosure statement

No potential conflict of interest was reported by the authors.



## Funding

This work was supported by Dumlupınar University [project number 20012/22].

## Supplemental data

The supplemental data for this article can be accessed at <http://dx.doi.org/10.1080/00958972.2015.1086997>.

## ORCID

Murat Taş  <http://orcid.org/0000-0002-2879-6501>

## References

- [1] J. Zuo, C. Bi, Y. Fan, D. Buac, C. Nardon, K.G. Daniel, Q.P. Dou. *J. Inorg. Biochem.*, **118**, 83 (2013).
- [2] M. Devereux, D. O'Shea, A. Kellett, M. McCann, M. Walsh, D. Egan, C. Deegan, K. Kędziora, G. Rosair, H. Müller-Bunz. *J. Inorg. Biochem.*, **101**, 881 (2007).
- [3] L.R. Kelland, N.P. Farrell, S. Spinelli, In *Uses of Inorganic Chemistry in Medicine*, N.P. Farrell (Ed.), pp. 109–134, The Royal Society of Chemistry (1999), .
- [4] M. McCann, B. Coyle, S. McKay, P. McCormack, K. Kavanagh, M. Devereux, V. McKee, P. Kinsella, R. O'Connor, M. Clynes. *BioMetals*, **17**, 635 (2004).
- [5] C. Deegan, B. Coyle, M. McCann, M. Devereux, D. Egan. *Chem. Biol. Interact.*, **164**, 115 (2006).
- [6] M. Gielen, E.R.T. Tiekink (Eds). *Metallotherapeutic Drugs and Metal-based Diagnostic Agents: The Use of Metals in Medicine*, Wiley, England (2005). <http://onlinelibrary.wiley.com/doi/10.1002/0470864052.fmatter/pdf>
- [7] M. Devereux, M. McCann, D. O'Shea, M. O'Connor, E. Kiely, V. McKee, D. Naughton, A. Fisher, A. Kellett, M. Walsh, D. Egan, C. Deegan. *Bioinorg. Chem. Appl.*, **2006**, 1 (2006). <http://www.hindawi.com/journals/bca/2006/080283/abs/>
- [8] L. Jia, J. Shi, Z.H. Sun, F.F. Li, Y. Wang, W.N. Wu, Q. Wang. *Inorg. Chim. Acta*, **391**, 121 (2012).
- [9] M. Porchia, A. Dolmella, V. Gandin, C. Marzano, M. Pellei, V. Peruzzo, F. Refosco, C. Santini, F. Tisato. *Eur. J. Med. Chem.*, **59**, 218 (2013).
- [10] L. Ronconi, P.J. Sadler. *Coord. Chem. Rev.*, **251**, 1633 (2007).
- [11] M.A. Azuine, H. Tokuda, J. Takayasu, F. Enjyo, T. Mukainaka, T. Konoshima. *Pharmacol. Res.*, **49**, 161 (2004).
- [12] T.D. Ashton, K.M. Aumann, S.P. Baker, C.H. Schiesser, P.J. Scammells. *Bioorg. Med. Chem. Lett.*, **17**, 6779 (2007).
- [13] P. Cui, T.L. Macdonald, M. Chen, J.L. Nadler. *Bioorg. Med. Chem. Lett.*, **16**, 3401 (2006).
- [14] K. Nomiya, R. Noguchi, K. Ohsawa, K. Tsuda, M. Oda. *J. Inorg. Biochem.*, **78**, 363 (2000).
- [15] V. Mathew, J. Keshavayya, V.P. Vaidya. *Eur. J. Med. Chem.*, **41**, 1048 (2006).
- [16] R.M. Mohareb, F. Al-Omran. *Steroids*, **77**, 1551 (2012).
- [17] H.H. Hammud, G. Nemer, W. Sawma, J. Touma, P. Barnabe, Y. Bou-Mouglabey, A. Ghannoum, J. El-Hajjar, J. Usta. *Chem. Biol. Interact.*, **173**, 84 (2008).
- [18] T. Theophanides, J. Anastassopoulou. *Rev. Oncol. Hematol.*, **42**, 57 (2002).
- [19] T.F. Kagawa, B.H. Geierstanger, A.H. Wang, P.S. Ho. *J. Biol. Chem.*, **266**, 20175 (1991).
- [20] C. Marzano, M. Pellei, F. Tisato, C. Santini. *Anti-Cancer Agents Med. Chem.*, **9**, 185 (2009).
- [21] C. Santini, M. Pellei, V. Gandin, M. Porchia, F. Tisato, C. Marzano. *Chem. Rev.*, **114**, 815 (2014).
- [22] L. Wang, Z. Wang, E. Wang. *J. Coord. Chem.*, **57**, 1353 (2004).
- [23] S.-I. Noro, S. Kitagawa, M. Yamashita, T. Wada. *J. Chem. Soc., Chem. Commun.*, **3**, 222 (2002). <http://pubs.rsc.org/en/content/articlelanding/2002/cc/b108695b/unauth#.divAbstract>
- [24] G.A. van Albada, S. Gorter, J. Reedijk. *Polyhedron*, **18**, 1821 (1999).
- [25] M. Devereux, M. McCann, V. Leon, V. McKee, R.J. Ball. *Polyhedron*, **21**, 1063 (2002).
- [26] W.-Z. Wang, X. Liu, D.-Z. Liao, Z.-H. Jiang, S.-P. Yan, G.-L. Wang. *Inorg. Chem. Commun.*, **4**, 327 (2001).
- [27] H. Xu, N. Zheng, H. Xu, Y. Wu, R. Yang, E. Ye, X. Jin. *J. Mol. Struct.*, **597**, 1 (2001).
- [28] E.E. Sileo, A.S. de Araujo, G. Rigotti, O.E. Piro, E.E. Castellano. *J. Mol. Struct.*, **644**, 67 (2003).
- [29] M.P. Brandi-Blanco, D. Choquesillo-Lazarte, J.M. González-Pérez, A. Castiñeiras, J. Niclós-Gutiérrez. *Z. Anorg. Allg. Chem.*, **631**, 2081 (2005).
- [30] J.J. Perry, G.J. McManus, M.J. Zaworotko. *J. Chem. Crystallogr.*, **34**, 877 (2004).

- [31] I. Bratsos, A. Bergamo, G. Sava, T. Gianferrara, E. Zangrando, E. Alessio. *J. Inorg. Biochem.*, **102**, 606 (2008).
- [32] B.S. Creaven, D.A. Egan, K. Kavanagh, M. McCann, M. Mahon, A. Noble, B. Thati, M. Walsh. *Polyhedron*, **24**, 949 (2005).
- [33] B.S. Creaven, M. Devereux, D. Karcz, A. Kellett, M. McCann, A. Noble, M. Walsh. *J. Inorg. Biochem.*, **103**, 1196 (2009).
- [34] B.S. Creaven, D.A. Egan, D. Karcz, K. Kavanagh, M. McCann, M. Mahon, A. Noble, B. Thati, M. Walsh. *J. Inorg. Biochem.*, **101**, 1108 (2007).
- [35] L. Mao, Y. Wang, Y. Qi, M. Cao, C. Hu. *J. Mol. Struct.*, **688**, 197 (2004).
- [36] O.V. Dolomanov, Luc J. Bourhis, R.J. Gildea, J.A.K. Howard, H. Puschmann. *J. Appl. Crystallogr.*, **42**, 339 (2009).
- [37] G.M. Sheldrick. *SHELX Acta Cryst.*, **A64**, 112 (2008).
- [38] L. Puntus, V. Zolin, V. Kudryashova. *J. Alloy Compd.*, **374**, 330 (2004).
- [39] Z. Vargová, V. Zeleňák, I. Čisárová, K. Györyová. *Thermochim. Acta*, **423**, 149 (2004).
- [40] K. Nakamoto. *Infrared and Raman Spectra of Inorganic and Coordination Compounds*, 5th Edn, Wiley Interscience, New York (1997).
- [41] D. Krajčiová, M. Melník, E. Havránek, A. Forgáčsová, P. Mikuš. *J. Coord. Chem.*, **67**, 1493 (2014).
- [42] W.A. Wani, Z. Al-Othman, I. Ali, K. Saleem, M.-F. Hsieh. *J. Coord. Chem.*, **67**, 2110 (2014).
- [43] J. Li, L. Jiang, S. Li, J. Tian, W. Gu, X. Liu, S. Yan. *J. Coord. Chem.*, **67**, 3598 (2014).
- [44] L. Subha, C. Balakrishnan, S. Thalamuthu, M.A. Neelakantan. *J. Coord. Chem.*, **68**, 1021 (2015).
- [45] J. Zhao, K. Peng, Y. Guo, J. Zhang, D. Zhao, S. Chen, J. Hu. *J. Coord. Chem.*, **67**, 2344 (2014).